buildings

MDPI

Article

Smart Materials for Zero Additional Energy: Europium- and Dysprosium-Doped Strontium Aluminate for Low-Level Artificial Light at Night

Ikechukwu Ogwu [1], Francis O. Okeke [2,*], Du-Min Kuang [3], Chika L. Onwuasoanya [4], Chijioke C. Onwuzuligbo [5] and Moses M. Okonkwo [6]

[1] International Education School, Hunan Institute of Engineering, Xiangtan 411104, China; ogwu@hnie.edu.cn
[2] Sustainable Engineering and the Built Environment Section, Canterbury Christ Church University, Canterbury CT1 1 QU, UK
[3] College of Mechanical Engineering and Mechanics, Xiangtan University, Xiangtan 411105, China
[4] Faculty of Environmental Sciences, Nasarawa State University, Keffi 1022, Nigeria
[5] Department of Architecture, Chukwuemeka Odumegwu Ojukwu University, Uli 431124, Nigeria
[6] Department of Architecture, Nnamdi Azikiwe University, Awka 420110, Nigeria
* Correspondence: f.okeke142@canterbury.ac.uk

Abstract

The integration of information technology in the built environment is intended to enable the efficient use of energy without compromising the comfort of humans. However, these devices and systems require a constant supply of energy, adding to the already high demand. In an attempt to promote zero additional energy-demand practices, this study explores the application of the direct and reversible property of smart photoluminescent material in the generation of artificial light at night (ALAN), where low-level light (LLL) is required for the identification of hazards. To achieve this, the energy transformation capacity of europium- and dysprosium-doped strontium aluminate ($SrAl_2O_4$:Eu^{2+}, Dy^{3+}) in the generation of visible light via photoluminescence was investigated. The performance of the material as a photoluminescent (PL) tape and component in PL paint was documented after activation by sunlight, inspired by evaluation tests and the Standard Test Method for Photopic Luminance of Photoluminescent Markings. From the single preliminary observation, tape luminance from initial tests in August 2020 declined from derived 8550 mcd/m^2 to 3150 mcd/m^2 at 10 min and 60 min respectively; then in September 2021, from derived 11,700 mcd/m^2 to 4500 mcd/m^2 at 10 min and 60 min respectively, after an additional tape layer was applied in a separate campaign. The 10- and 60 min checkpoints evaluate how well the tape holds its brightness over time. For the paint, symbol recognition remained visible up to 90 min and became indistinct after 120–150 min after activation, supporting qualitative symbol discernibility under the stated test conditions. The coating dried hard in 25 min, set to touch in 12 h, and retained afterglow after 24 h water immersion and exposure to 0 °C and 42 °C. These exploratory, non-replicated results demonstrate persistent afterglow and qualitative symbol discernibility under the stated laboratory conditions and support further controlled evaluation for low-light built-environment applications.

Keywords: smart materials; energy sustainability; artificial light at night (ALAN); photoluminescence; europium- and dysprosium-doped strontium aluminate ($SrAl_2O_4$:Eu^{2+}, Dy^{3+})

Check for updates

Academic Editor: Lambros T. Doulos

Received: 27 July 2026
Revised: 28 October 2026
Accepted: 30 October 2026
Published: 2 November 2026

Copyright: © 2026 by the authors. Licensee MDPI, Basel, Switzerland. This article is an open access article distributed under the terms and conditions of the Creative Commons Attribution (CC BY) license.

1. Introduction

The primary notion of "smart" in discussions around materials used in the built environment is centered on responsiveness—the capacity of a material to undergo a direct, physical change when exposed to a specific environmental stimulus (e.g., light, temperature, humidity, stress), and to stabilize or revert as conditions change [1]. This concept has gained prominence because it offers a demand-side route to lower energy use: instead of relying solely on continuously electrically powered devices and controls, performance improvements can be embedded in the intrinsic properties of the material itself [2]. In the context of smart cities and refurbishment, a chemistry-led "innovation package" is presented as a practical pathway to improved building energy efficiency through deployable products and systems suited to existing building stock [3]. Building-performance studies similarly argue that smart materials can act as a functional "second skin", enhancing envelope behavior and reducing operational energy and related emissions through improved thermal and environmental moderation [4]. From a sustainable-architecture standpoint, smart materials are framed as engineered materials whose properties can be altered by external stimuli; here, material selection becomes a primary lever for energy-conscious design [5,6]. Importantly for the present study, material-led strategies have been extended to passive lighting-related functions, including photoluminescent and "cool" coatings proposed to contribute to outdoor nighttime visibility while simultaneously lowering cooling and lighting energy demand [7]. Photoluminescent (PL) materials are reported in the literature as requiring no electricity, wiring, or batteries once charged; as non-toxic, non-radioactive, and non-explosive; and as offering a typical service lifetime exceeding 30 years, though these properties are drawn from manufacturer and prior-study data rather than tested directly in the present work [7]. More broadly, recent sustainable building-performance research has emphasized transparent evaluation practices and reliability when emerging technologies are assessed for sustainability applications [8].

Despite decades of efficiency gains, the global energy system remains heavily dependent on fossil-fuel combustion, with coal, oil and natural gas still supplying the majority of primary energy. In electricity production, coal continues to be the single largest source, with 37% of global electricity coming from coal-fired plants [9], and artificial lighting accounting for roughly 15% of this, resulting in about 5% of greenhouse-gas emissions [10,11]. Recent work has also targeted daylighting and energy performance jointly through optimized shading strategies [12,13], reinforcing the broader case for material- and design-led approaches to reducing lighting-related energy demand. Accordingly, reducing electricity demand for lighting can deliver dual benefits: lowering fossil-fuel use and emissions, while also helping to mitigate electric light pollution, particularly artificial light at night (ALAN), which is increasingly linked to adverse human health outcomes. ALAN, perceived to play an essential role in the appeal and safety of indoor as well as outdoor spaces, also impedes sleep and biological processes [14–16]. This is because ALAN causes disruptions in the natural light cycle in spaces, at periods, and with brightness that is not consistent with natural patterns that keep the human circadian rhythm in check [17,18]. Currently, over 75% of the world's population is exposed to ALAN, with light exposure levels twice as high between sundown and sleep, when compared against total exposure to natural light during the day [19]. This increased exposure delays sleep, reduces melatonin synthesis, and impairs next-morning alertness [20,21]. While advances in artificial lighting technology have led to decreased costs, it has at the same time, increased illumination levels, with the use of light in areas and spaces that were hitherto not lit [22], or where natural night light would have been sufficient. In fact, regardless of ambient conditions, artificial light is used as much, and for as long as is available; it is now common to leave lights on overnight, even when not in use [23]. This practice has been growing at a rate of 3 to 6% per year

since the second half of the 20th century [24], and as a result, the world has experienced widespread loss of the night and substantially modified light–dark cycles in most developed countries [25]. To curb this practice, intelligent control systems have been proposed, with features that automatically power on only at night, or when there is motion in a given space. However, these systems comprise electronic components which still require power, and no matter how small or direct they may be, electricity must still be supplied [1]. For instance, with emergency exit markings, an important and legally required feature in non-residential buildings, needed to provide low-level light for safe evacuation in an emergency, electricity is required 24 h a day and 365 days a year to keep them running, and several of them are required for each floor of a building and for several buildings. These signs are kept on no matter the time of day, and are required to also have a backup battery in case of an emergency [26,27]. Larger facilities will integrate intelligent software management systems to monitor all exit signs and automatically notify the facility manager when a connected sign fails. This intelligent management system requires electric exit signs with networking capability, and the installation of wired or wireless networking as well as computer systems [27].

Although policy and practice increasingly acknowledge luminous/photoluminescent egress-path marking as a viable safety strategy in high-rise and complex buildings, adoption in the built environment still depends on credible, application-oriented evidence. For example, code provisions for luminous egress-path markings specify where such systems are required and how they should delineate steps, handrails, and perimeter demarcations in exit enclosures, reflecting growing institutional confidence in "self-luminous" guidance systems [28]. At the same time, emergency lighting and exit-marking regimes continue to be framed around continuous availability during power loss (commonly 90 min); a requirement that drives the continued dependence of conventional solutions on electricity, batteries, testing, and maintenance, even where lighting is only needed at low levels for wayfinding and hazard avoidance [29]. However, the peer-reviewed research base that can guide designers and facility managers in choosing between electrically powered nighttime lighting and photoluminescent alternatives remains fragmented [30]. Much of the existing work on photoluminescent systems emphasizes materials development or single-use demonstrations (e.g., coatings formulated for safety marking using acrylic-based systems, or long-afterglow aluminates explored in road-marking contexts) [31], but far fewer studies translate these advances into building-relevant performance claims expressed in standardized metrics that practitioners recognize [32]. In particular, there is limited literature that simultaneously (i) quantifies afterglow performance using recognized photopic luminance procedures, (ii) provides evidence of visibility claims for reported hazard identification and wayfinding tasks, and (iii) checks durability under basic environmental exposures that influence serviceability in real buildings. This matters because standards such as ASTM E2073 exist precisely to enable comparable photopic luminance evaluation of photoluminescent markings, yet published building-focused studies do not consistently report outcomes in ways that directly support specification and deployment decisions [33]. Unlike acrylic-based safety-marking coatings and long-afterglow aluminate road-marking systems, which are typically validated for surface durability or color retention alone, and unlike polyester-resin PL signage, the present study combines acrylic-binder durability screening with standards-inspired photopic decay and task-based visibility testing in a single building-relevant evaluation.

This study attempts to address these gaps through an exploratory, application-oriented evaluation of europium- and dysprosium-doped strontium aluminate ($SrAl_2O_4$:Eu^{2+},Dy^{3+}) in two delivery formats: adhesive-backed PL tape and acrylic-binder PL paint. The objective is to characterize afterglow decay, assess qualitative symbol discernibility under

controlled total-darkness conditions, and conduct preliminary water- and temperature-resistance screening relevant to built-environment applications. The study makes three specific contributions: (1) it reports time-dependent illuminance and approximate derived luminance for PL tape using a standards-inspired evaluation procedure; (2) it documents the qualitative discernibility of a paint-based symbol at a fixed viewing distance under defined conditions; and (3) it combines photometric, task-based and preliminary environmental screening within a single built-environment-oriented assessment. The novelty therefore lies in this integrated application-focused evaluation rather than in the use of an acrylic binder alone. The experiments are preliminary and non-replicated and should not be interpreted as specification-grade validation or as direct evidence of energy or ALAN reduction in operational buildings.

2. Materials and Methods

The evaluation approach for the current study was inspired by the DOT/FAA/AM-98/2 (performance demonstration of zinc sulfide and strontium aluminate photoluminescent floor proximity escape path marking systems) [34], DOT/FAA/AR-TN09/35 (photoluminescent material evaluation) [35], testing of photoluminescent materials of the US Department of Transportation, Federal Aviation Administration [36] and the Standard Test Method for Photopic Luminance of Photoluminescent (Phosphorescent) Markings (ASTM E2073) [33] as contained in the Photoluminescent Lighting Council Standards.

Experimental Scope

The present work was designed as an exploratory screening study in a controlled environment. One tape-covered canvas specimen was evaluated in each tape campaign, with one time-series measurement sequence per campaign. The paint visibility assessment used one prepared symbol specimen and one observation sequence. The water-immersion and temperature-resistance assessments were conducted as single, non-repeat preliminary tests on the prepared paint specimen. No independent specimen-level replication was undertaken. Further, because the testing room lacked specialized optical sealing and anti-reflective coatings, the environment was subject to potential ambient stray light. However, measurements were under zero active internal illumination—all active natural and artificial light sources were eliminated. Any residual ambient low-energy stray light would require prolonged exposure to saturate the electron traps.

Commercially available PL material was obtained as strontium aluminate phosphor powder and adhesive-backed vinyl tape. The tape was supplied ready to use, while a water-soluble flat acrylic binder was chosen to be mixed with the powder and water in preparing the PL paint. PL paint usually contains a PL powder chosen from a group of chemically doped metal sulfides, alkaline earth metal aluminates and alkaline earth metal silicates, as well as a binder chosen from a group comprising mineral gypsum, calcium sulfate hemihydrates or methyl methacrylate/acrylic that can harden when mixed with water [37,38]. PL materials present a day color of light green, similar to light aventurine green powder or mint green. They can glow in the dark for over 12 h after excitation by D65 standard light source—artificial day light at 1000 lx luminous flux density for 10 min, meet the US requirement of ASTM F963-16 (Standard Consumer Safety Specification on Toy Safety) [39], Test Method CPSC-CH-E1003-09.1 for total lead, and ASTM F 963-16 (Clause 8.3) for soluble heavy metal; and is registered for EU REACH standard in accordance with the REACH regulation (EC) No 1907/2006 [40]. The percentages of binder mix to PL powder can vary depending on the desired use and longevity of the application. A mix ratio of 5:2:2 by mass, i.e., 5 parts PL powder, 2 parts water, and 2 parts binder, was prepared for the paint composition in the current study. Thus, 25 g of PL powder was put into a

glass beaker, followed by 10 g of water and 10 g of the binder, and mixed manually before application with a painter's brush.

The resulting composition was first monitored according to a surface drying test in line with the ASTM D 5895-01 [41] Standard Test Methods for Measuring Times of Drying or Curing During Film Formation of Organic Coatings Using Mechanical Recorders, and according to GB/T1728-2002 [42]. The test, in part, describes the 'set-to-touch' time as the condition when the paint has solidified sufficiently by solvent evaporation or chemical reaction or both, that it no longer flows or sticks to a finger that slightly touches it. To avoid conflating distinct drying and curing terms, the 25 min observation is reported here as the recorded dry-hard response and the 12 h observation as the later touch assessment; neither is interpreted as a complete characterization of final curing.

Next, a water-resistance test in line with ASTM D 870-02 [43] Standard Practice for Testing Water Resistance of Coatings Using Water Immersion, and according to GB/T1733-1993 [44], was conducted to determine durability; the prepared paint was wholly immersed in water in a corrosion-resistant container at room temperature for 24 h, as described also in Bi et al. [45]. Water permeates the coating at rates that are dependent upon the characteristics of the coating and upon the temperature of the water. Effects such as color change, blistering, loss of adhesion, softening, or embrittlement were observed and documented. Immediately after, low- and high-temperature-resistance tests were then performed by exposing the paint to a constant temperature of 0 °C for 24 h and 42 °C for 6 h.

Further, evaluation tests inspired by DOT/FAA/AR-TN09/35 were conducted on the prepared PL paint to assess qualitative symbol discernibility under optimal ambient low-light conditions. In this evaluation, a 5 cm × 5 cm letter 'A' was drawn onto a 10 cm × 10 cm white cardboard paper (see Figure 1). The letter was unpainted while the rest of the paper was covered with prepared PL paint, then exposed to outdoor sunlight for 6 h (12:00–18:00), and then quickly transferred to a simulated darkened location without natural or artificial light. The symbol was observed from a distance of 450 cm (see Figure 2) and photographed with a Samsung SM-N950U camera manufactured by the SEVT – Samsung Electronics Vietnam Thai Nguyen factory (aperture F1.7, focal length 4.30 mm, ISO 50) at 0, 10, 20, 30, 40, 50, 60, 90, 120 and 150 min. Camera exposure was locked, and the device position was maintained; images were not enhanced. This was a single-symbol qualitative demonstration under total-darkness conditions and does not establish general wayfinding or hazard-recognition performance across different symbols, observers, viewing angles, backgrounds or ambient-light conditions [35,36].

For the photometric test, the PL adhesive-backed tape was exposed to sunlight in an open area. The adhesive-backed tape was applied to a 40 cm × 50 cm (0.4 m × 0.5 m; area = 0.20 m^2) canvas, and exposed to sunlight for 6 h (from 12 noon to 6 pm). The material was then quickly taken to a simulated darkened location without natural or artificial light. The performance of the material was monitored for 5 h, from 6 pm to 11 pm. Because a dedicated luminance meter was unavailable, the surface luminance (L) in cd/m^2, of the PL tape was calculated from the experimental illuminance (E) data collected by a commercially available handheld and portable TES 1330A digital lux (lx) meter, made in Taiwan. This calculation relies on the point-source approximation derived from the photometric inverse-square law, expressed as:

$$L = \frac{E \times d^2}{A} \quad (1)$$

where d is the distance from the source to the sensor plane, and A is the precise surface area of the emitter [34]. For this study, the emitter is the PL tape-covered flat 0.20 m^2 canvas surface at a testing distance of 3 m, to satisfy the far-field criteria defined by CIE S 025/E:2015 [46], and to eliminate structural geometry errors from the area source [38]; this is also inspired

by [35]. For conversion of measured illuminance to approximate derived luminance, the PL tape was treated as a Lambertian emitter. This was a modeling assumption rather than an experimentally demonstrated surface property. Spatially uniform appearance does not by itself establish Lambertian angular emission, and angular dependence was not measured in the present study. This assumption potentially overestimates obstacle brightness at close-up, normal viewing angles due to specular reflections, while underestimating it at distant, grazing angles due to internal light trapping. Consequently, the calculated luminance values should be interpreted as approximate derived luminance rather than direct luminance measurements. Illuminance was measured using a TES 1330A digital lux meter, which is specified with an accuracy of ±3% of reading, ±0.5% of full scale below 10,000 lx and has a nominal measuring range of 0.01–200,000 lx. At the lowest measured illuminance levels of 0.05–0.08 lx, the full-scale contribution to instrument uncertainty is of the same order as the measured values. These late-stage readings therefore do not support high-precision quantitative luminance estimation. Increased brightness was initially observed in tape overlap areas during testing in August 2020, which was accompanied by a higher recorded surface luminance; however, irradiance was not measured in either campaign, so the datasets are not directly comparable. Ambient environmental conditions were monitored throughout the sunlight activation phase using a digital thermo-hygrometer clock (model HTC-2). The device logged air temperature (measurement range: −10 °C to +50 °C, accuracy: ±1 °C) and relative humidity (measurement range: 10% to 99% RH, accuracy: ±5% RH) concurrently with a real-time digital clock display. However, because the HTC-2 does not log solar irradiance, the afternoon solar profiles were correlated with clear-sky solar elevation models for the region. The ultraviolet (UV) index reached an estimated clear-sky peak of 10 (very high) during the solar noon window before declining.

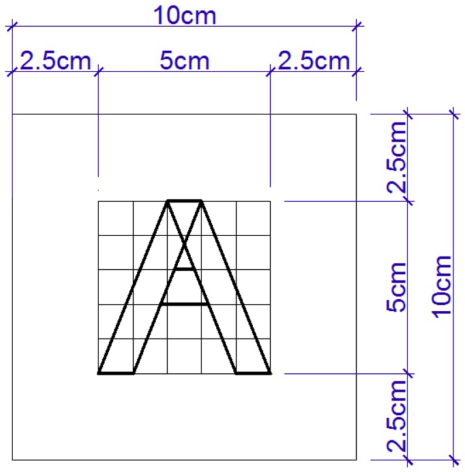


Figure 1. Prepared letter 'A' for inspired visibility test (authors).

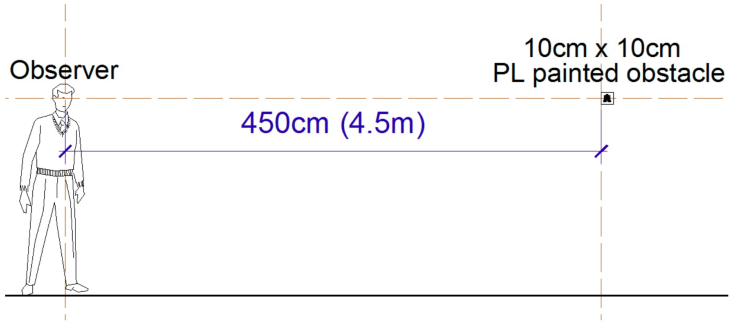


Figure 2. Inspired visibility test setup (authors).

The August 2020 values originated from the initial tape trial: measured illuminance was 0.24 lx immediately after activation and 0.05 lx at 240 min, corresponding to approximate derived luminance of 10,800 and 2250 mcd/m^2. The September 2021 values originated from the double-layer dataset reported in Table 1: measured illuminance was 0.90 lx immediately after activation and 0.05 lx at 240 min, corresponding to approximate derived luminances of 40,500 and 2250 mcd/m^2. Photographic evidence was also captured with the mobile phone SM-N950U camera, maintaining a distance of 300 cm (3 m) from the target. The values were recorded at intervals of 0 min (immediately after exposure), 10 min, 20 min, 30 min, 40 min, 50 min, 60 min, 90 min, 120 min, 240 min, and 300 min.

Table 1. Photometric test results.

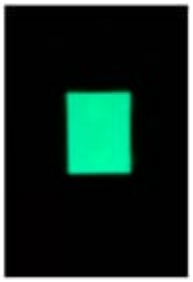
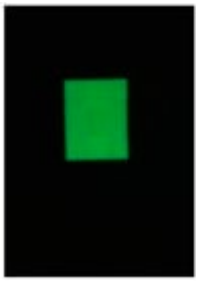
Date: September, 2021		Temperature: 31 °C		Humidity: 60%	
UV index: Very high (10)		Activating light: Outdoor Sun		Exposure time: 6 h	
Captured image					
Time (pm)	n/a	6:00	6:10	6:20	6:30
* D (mins)	n/a	0	10	20	30
** E (lx)	n/a	0.90	0.26	0.22	0.18
1/√illum′	n/a	1.05	1.96	2.13	2.36
*** L (cd/m^2)	n/a	40.50	11.70	9.90	8.10
mcd/m^2 = L × 1000	n/a	40,500	11,700	9900	8100
Captured image					
Time (pm)	6:40	6:50	7:00	7:30	8:00
D (mins)	40	50	† 60	† 90	† 120
E (lx)	0.16	0.15	0.10	0.08	0.07
1/√illum′	2.50	2.58	3.16	3.54	3.78
L (cd/m^2)	7.20	6.75	4.50	3.60	3.15
mcd/m^2 = L × 1000	7200	6750	4500	3600	3150

Table 1. *Cont.*

Captured image				-	-
Time (pm)	9:00	10:00	11:00	-	-
D (mins)	† 180	† 240	† 300	-	-
E (lx)	0.06	0.05	0.05	-	-
1/√illum′	4.08	4.47	4.47		
L (cd/m^2)	2.70	2.25	2.25	-	-
mcd/m^2 = L × 1000	2700	2250	2250		

* D represents duration. ** E represents single illuminance. *** L represents derived luminance. n/a means not applicable. † Illuminance ≤0.10 lx, of the same order as the meter's full-scale uncertainty term.

3. Results

The September 2021 tape dataset showed a rapid initial decrease in measured illuminance followed by a slower decay. Approximate derived luminance decreased from 40,500 mcd/m^2 immediately after activation to 11,700 mcd/m^2 at 10 min, 4500 mcd/m^2 at 60 min and approximately 2250 mcd/m^2 at 240–300 min (Figure 3; Table 1). The transformed variable $1/\sqrt{E}$ showed an approximately linear relationship with elapsed time, described by $1/\sqrt{E} = 2.05 + 0.0101t$ ($R^2 = 0.82$) (Figure 4). This linearized relationship is presented as a descriptive fit to the non-replicated dataset rather than as definitive validation of a universal decay model. Brighter appearance was observed in overlapped tape regions; however, because the single- and double-layer datasets were obtained in separate campaigns without measured solar irradiance, this observation cannot establish a controlled layer-thickness effect.

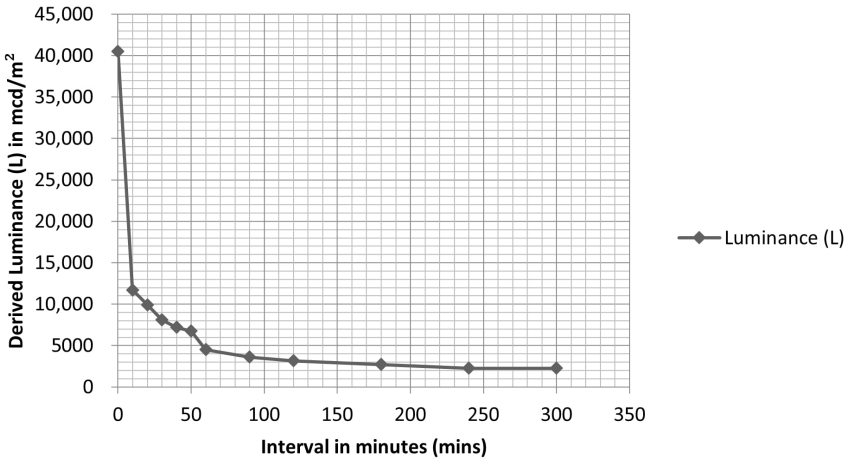


Figure 3. Phosphorescence emission decay of adhesive-backed strontium aluminate PL tape over time.

For the paint visibility test, qualitative discernibility of the single letter 'A' was assessed from 450 cm in a simulated dark room. The symbol remained distinguishable through

90 min and became indistinct at 120–150 min (Table 2). This result applies only to the single symbol, viewing geometry and total-darkness conditions used and should not be interpreted as validated wayfinding or generalized hazard-identification performance.

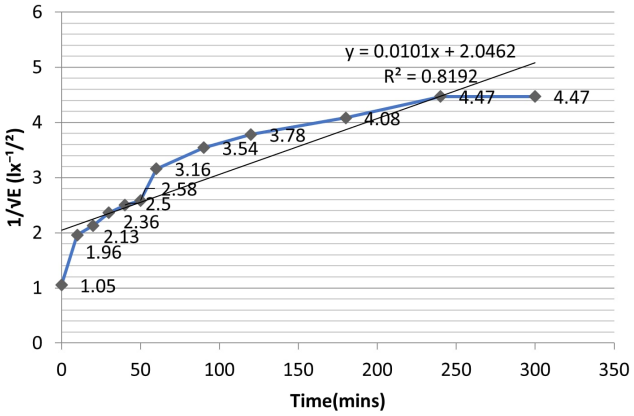


Figure 4. Linearized plot of $1/\sqrt{E}$ against elapsed time for the September 2021 PL tape dataset. Linear regression: $1/\sqrt{E} = 2.05 + 0.0101t$, $R^2 = 0.82$.

Table 2. Visibility test results.

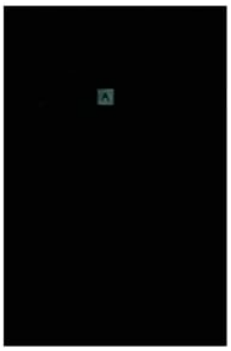
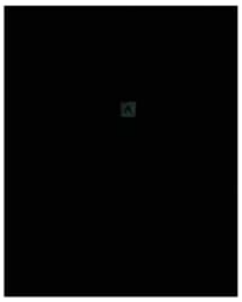
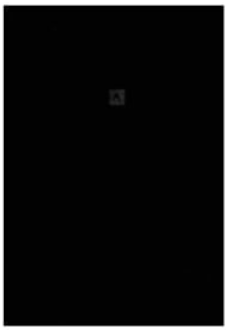
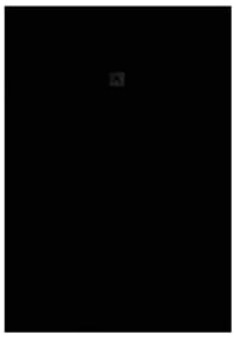
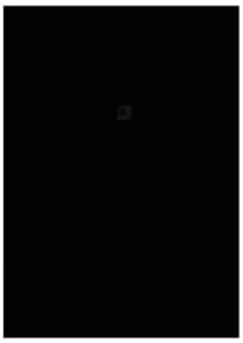
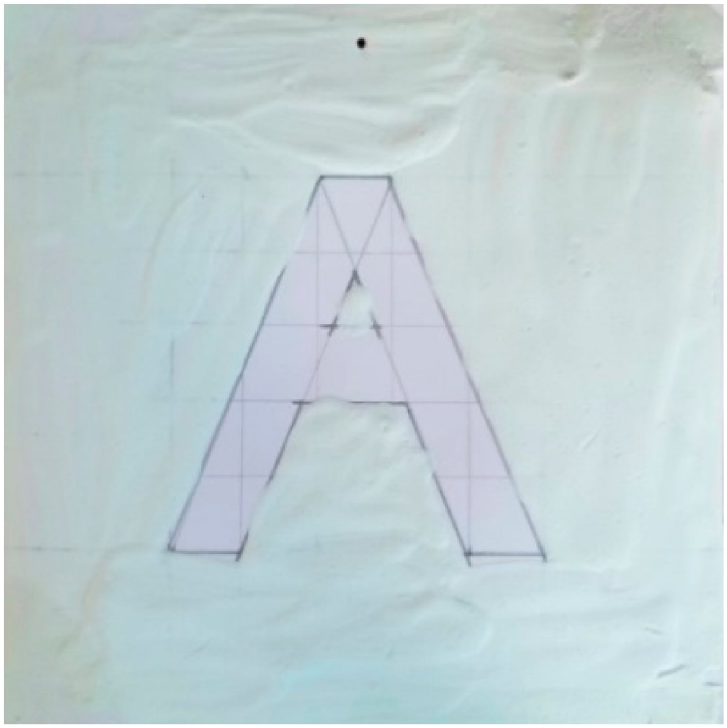
Date: September, 2021		Temperature: 37–25 °C	
Humidity: 60%		UV index: Very high (10)	
Activating light: Outdoor Sun		Exposure time: 6 h	
Captured image			
Time (pm)	Pre-charge	6:00	6:10
Duration (mins)	Pre-charge	0	10
Remarks	n/a	Visible	Visible
Captured image			
Time (pm)	6:20	6:30	6:40
Duration (mins)	20	30	40
Remarks	Visible	Visible	Visible

Table 2. *Cont.*

Captured image			
Time (pm)	6:50	7:00	7:30
Duration (mins)	50	60	90
Remarks	Visible	Visible	Visible
Captured image			-
Time (pm)	8:00	8:30	-
Duration (mins)	120	150	-
Remarks	Indistinct visibility	Indistinct visibility	-

A single non-repeat preliminary environmental screening was conducted on the prepared PL paint made from an author-defined mix of 55.56% $SrAl_2O_4$:Eu^{2+},Dy^{3+} phosphor powder, 22.22% binder and 22.22% water. The distinct daytime and nightime visual characteristics of the paint applied on the prepared letter A prior to durability tests is shown in Figure 5. During preliminary drying observations, the coating exhibited the recorded dry-hard response at approximately 25 min, while a later touch assessment was recorded at 12 h. These observations are not interpreted as a complete characterization of final curing. The same specimen was used for the short-duration water- and temperature-resistance screenings described below.

The fundamental principle and operating procedure for testing the water resistance of coatings according to ASTM D 870-02 and GB/T1733-1993 standards is the partial or complete immersion of coated specimens in distilled or demineralized water at ambient or elevated temperatures. Although the apparatus and procedure could be employed in immersion tests using solutions of various materials in water, this practice is limited to tests in water alone. Thus, for this experiment, the paint was wholly immersed in water in a container that is resistant to corrosion at room temperature, as shown in Figure 6a, for 24 h. After the water was decanted, the sample was activated by a mobile phone flashlight of 60 lx at a horizontal distance of 45 cm for 1 min. It was observed that there was no color change, no blistering, no softening, and no embrittlement on the paint. The paint also retained its afterglow immediately after activation for 1 min, as shown in Figure 6b,c.



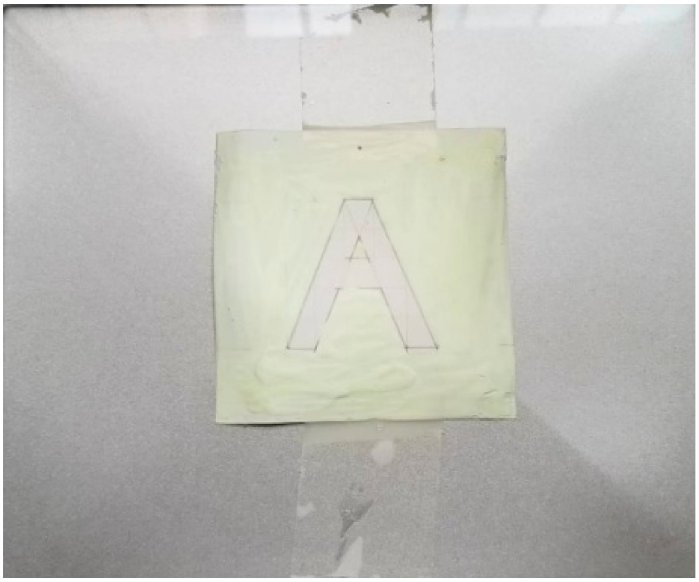
(**a**)



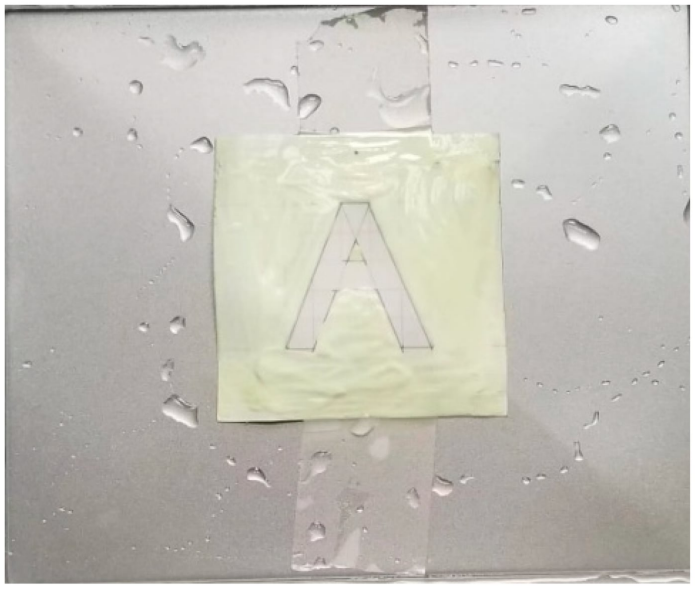
(**b**)

Figure 5. Daytime (**a**) and nighttime (**b**) appearance of the paint before durability tests.

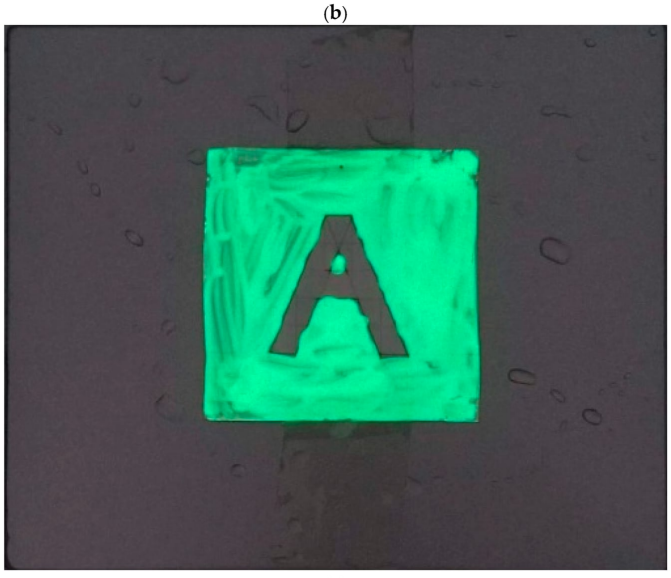
The sample was subjected to a high-temperature exposure at 42 °C for 6 h and a low-temperature exposure at 0 °C for 24 h using a portable room heater and refrigeration unit, respectively (Figure 7a,b). After subsequent activation with a mobile phone flashlight, no visible adverse effect was observed under the stated screening conditions: no peeling, cracking, shedding or discoloration was evident, and afterglow remained observable (Figure 7c). Because the test used a single specimen and short exposure periods, these observations do not establish long-term durability or serviceability.



(**a**)



(**b**)

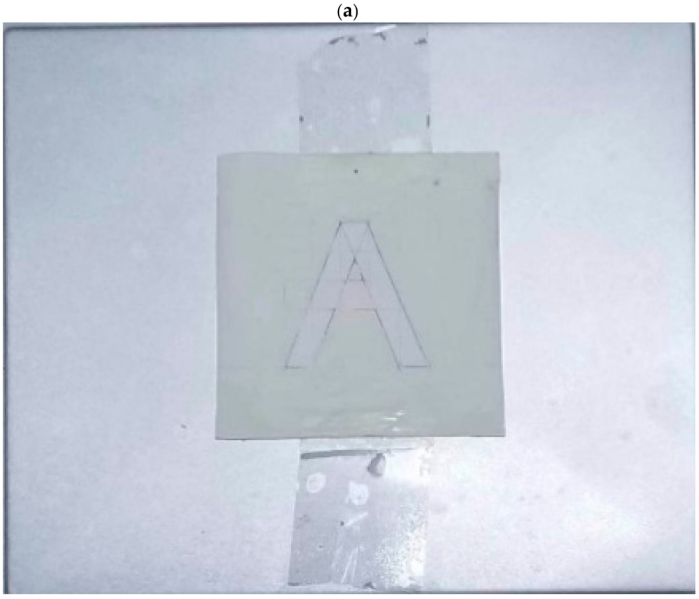


(**c**)

Figure 6. Fully immersed sample in water for 24 h (**a**), sample after decantation (**b**) and after activation for 1 min (**c**).



(**a**)



(**b**)



(**c**)

Figure 7. Preliminary temperature-resistance screening of the PL paint: (**a**) high-temperature exposure at 42 °C for 6 h; (**b**) low-temperature exposure at 0 °C for 24 h; and (**c**) afterglow observation following the temperature exposures and subsequent 1 min activation.

4. Discussion

This exploratory study assessed whether commercially available $SrAl_2O_4:Eu^{2+},Dy^{3+}$ could provide persistent low-level photoluminescent output in two built-environment delivery formats: adhesive-backed PL tape and acrylic-binder PL paint. The evidence comprises a non-replicated tape photometric decay assessment, a single-symbol qualitative paint visibility test and preliminary single-specimen environmental screening; interpretation is therefore limited to the stated experimental conditions.

4.1. Afterglow Behavior and Decay Kinetics

Across both PL formats, the key performance signature is a fast initial decay followed by a longer, weaker tail, which is consistent with how persistent phosphors discharge stored energy: shallow traps empty quickly after lights-out, while deeper traps sustain the longer afterglow at lower intensity. In the tape photometric monitoring, derived luminance decreased from 40,500 mcd/m^2 immediately after activation to 11,700 mcd/m^2 after 10 min (a 71.1% reduction from the initial value; 28.9% remaining). After this early drop, the decay became more gradual (i.e., 4500 mcd/m^2 at 60 min, while remaining detectable; 3600 mcd/m^2 at 90 min; and 2250 mcd/m^2 at 240–300 min, representing a 94.4% reduction). Practically, the 0 s initial burst and early drop is unreliable because of the sharp decline in the first few minutes. For this reason, commercial testing standards typically measure brightness at 10 min and 60 min, prioritizing long-term human visibility in real-world emergency egress over initial brightness values at deployment; the 10 min test point provides high visibility during evacuation rush, while the 60 min test point provides sustained glow for rescue teams. Also, the plot of $1/\sqrt{\text{Illuminance}}$ versus time was approximately linear, indicating that the decay is well described by a power-law/Becquerel-type relationship rather than a simple single-exponential fade; this is a useful finding because it supports extrapolation and comparison between charge conditions and material loadings. In addition, the observation that overlapped (double-layer) tape regions glowed brighter provides evidence of a direct design lever: increasing effective pigment thickness/area coverage increases initial luminance and is assumed to extend the period of functional visibility, which can be exploited in high-risk locations (e.g., step edges, door hardware zones, or obstacle perimeters) where contrast is more valuable than uniform glow [47].

4.2. Linking Afterglow to a Task: Hazard Identification and Legibility

Because the study targets hazard identification (rather than general visual comfort or broad-area illumination), the visibility test is central: it evaluates whether the PL emission can still create recognizable contrast for a simple symbol at a scaled viewing distance. The paint-based sample remained visible for up to 90 min post-charge, with visibility becoming indistinct after 120–150 min. This result aligns well with practical needs in many "low-level light" contexts (parks, pedestrian/cycle edges, corridors, or nighttime navigation zones) where the requirement is not high illuminance but just enough contrast to avoid obstacles and maintain directional confidence [48]. It also responds to an important implementation concern: in real settings, PL systems succeed when they support visual acquisition under adaptation-limited conditions (eyes transitioning from light to dark), which typically occurs over 20 to 30 min to an hour after darkness [49].

At the building-safety end of the application spectrum, luminous egress and low-location guidance systems are often specified using time-linked performance targets (commonly assessed at 10 and 60 min after lights-out under defined charging conditions). While this study did not capture luminance directly from a dedicated luminance meter, surface luminance in cd/m^2 was calculated based on the point-source approximation derived from the photometric inverse-square law. Notwithstanding, the task-based evidence shows that

the acrylic-bound PL paint maintained recognizable contrast through the 90 min window, and the PL tape retained a derived 4500 mcd/m^2 at 60 min, remaining detectable. Further, the strength of the current approach is that it bridges a frequent gap in the literature: many studies report claims of material brightness and decay but do not show or demonstrate whether the glow remains visible at a realistic viewing distance for visual tasks.

These visibility findings should be read within clear boundaries. Only one symbol (the letter "A"), one viewing distance (4.5 m) and a darkened environment were used; multiple symbols, observers, background luminances and viewing angles were not tested, so the result cannot be generalized to other signs or observation conditions. Real buildings are also rarely completely dark. Stray light from adjacent spaces, street lighting or passing vehicles raises background luminance, reduces the contrast between a glowing symbol and its surroundings, and is likely to shorten the time for which a sign remains identifiable. The 90 min discernibility reported here therefore represents a best-case laboratory condition rather than an expected in-service duration.

4.3. Comparing Tape and Acrylic-Binder Paint as Deployment Formats

A preliminary practical finding is that an acrylic binder can accommodate a high-loading $SrAl_2O_4$:Eu^{2+},Dy^{3+} coating while preserving visible afterglow after the short-term water and temperature screenings used here. The coating showed a recorded dry-hard response at approximately 25 min, while a later touch assessment was recorded at 12 h; these observations do not constitute a complete characterization of final curing, which is compatible with common refurbishment workflows where coatings can be applied off-hours and left to cure overnight. Following 24 h water immersion, the paint showed no blistering, softening, embrittlement, or loss of afterglow immediately after re-activation; similarly, exposure to 0 °C and 42 °C did not produce peeling, cracking, shedding, discoloration, or a noticeable reduction in afterglow. These durability indicators matter because PL coatings are only attractive as a sustainability strategy if they can survive cleaning regimes, humidity events, and seasonal temperature swings without performance collapse [50].

Compared with tape, the paint also offers wider application prospects: it can be applied to complex geometries (curbs, textured surfaces, stair nosings, columns, door surrounds), can be layered strategically, and can be integrated into retrofits without specialized fixtures. Tape retains advantages for rapid installation and predictable factory-controlled pigment distribution, but it is inherently limited by substrate adhesion performance, edge-lifting risks, and constrained geometry. The present results therefore support a differentiated deployment logic: use tape where speed and reversibility dominate (temporary works, quick demarcation, maintenance marking) and use acrylic-based PL paint where geometric flexibility dominates. While the research by Osmi et al. [51] demonstrates the use of polyester resin mixed with PL powder in making glow-in-the-dark emergency signage, the current study also indicates that an acrylic binder can retain visible afterglow under the short-term screening conditions used here. This product is intended for use with europium- and dysprosium-doped strontium aluminate ($SrAl_2O_4$:Eu^{2+},Dy^{3+}) pigment in the making of glow-in-the-dark paint, providing low-level artificial light at night for identification of hazards.

Acrylic-binder systems also carry potential disadvantages that were not evaluated here and should be weighed alongside their geometric flexibility. The paint used a high phosphor loading (55.56% by mass in the wet mix, and a higher pigment fraction in the dry film once water has evaporated). High solid contents of this kind can reduce coating cohesion and mechanical strength, increase porosity, and facilitate water-vapor penetration, with possible consequences for abrasion resistance, adhesion and long-term afterglow retention. Mechanical, porosity, permeability, adhesion and abrasion properties were not measured,

and the 24 h immersion and short thermal screenings cannot exclude such effects. Hand-brushed application may also give less uniform pigment distribution and film thickness than factory-produced tape, affecting repeatability. The greater geometric flexibility of the paint is therefore a potential advantage rather than a demonstrated superiority, and both formats' limitations should be considered when selecting between them.

4.4. Potential Relevance to ALAN Reduction and Zero-Additional-Operational-Energy Applications

The broader sustainability relevance of these findings is that they point to a credible demand-side lighting alternative for specific nighttime functions. The study does not argue that PL replaces all outdoor lighting or all emergency lighting; instead, it shows that in use-cases where illumination needs are intrinsically low (hazard outlining, path edge delineation, short-distance symbol recognition), PL can supply functional light without continuous electricity, batteries, wiring, or control overheads. This directly addresses a persistent weakness of "smart" lighting strategies that rely on sensors, networks, and standby power: even when energy use is reduced, the system still depends on electricity and maintenance, and it still adds to light emissions when it is active. In contrast, a passive PL system emits only after lights-out and then naturally decays, which can be beneficial in managing ALAN intensity and duration [1]. These two parameters are closely tied to ecological and human health concerns.

4.5. Limitations and Future Validation

Several limitations constrain interpretation of the present results. First, luminance was not measured directly; it was estimated from lux-meter illuminance using a photometric model and an assumed Lambertian-emitter approximation. The lowest 0.05–0.08 lx readings are of the same order as the meter's full-scale uncertainty term and therefore support only approximate late-stage derived luminance values. Second, the tape, visibility and environmental tests were not independently replicated, so variability and reproducibility could not be quantified. Third, the single- and double-layer tape datasets were collected in separate campaigns without measured solar irradiance, preventing a controlled comparison of layer thickness or excitation dose. Fourth, the visibility test involved one symbol under total darkness, and the water- and temperature-resistance assessments were short-duration single-specimen screenings; neither establishes general wayfinding performance nor long-term serviceability. Fifth, the visibility test excluded ambient stray light, which in real buildings raises background luminance, reduces contrast and is expected to shorten sign identification time. Sixth, the mechanical strength, porosity, water-vapor permeability, adhesion and abrasion resistance of the high-loading acrylic coating were not measured.

Future work should use direct luminance measurement, controlled optical excitation, replicated specimens, angular-emission characterization, systematic thickness comparisons, multiple-symbol/user visibility testing, accelerated and long-term durability protocols, and full-scale field trials that directly quantify any reductions in electrical lighting demand or ALAN exposure.

5. Conclusions

Buildings remain among the largest end-use energy consumers, making demand-side interventions an important route for reducing energy use and associated emissions. This study investigated the afterglow behavior and visibility potential of europium- and dysprosium-doped strontium aluminate ($SrAl_2O_4:Eu^{2+},Dy^{3+}$), applied as adhesive-backed PL tape and as a high-loading acrylic-binder PL paint. Under the specific experimental conditions employed, both forms exhibited sustained afterglow following initial activation. For the adhesive-backed PL tape, derived photometric measurements indicated persistent

emission for at least 120 min, with detectable afterglow continuing beyond this period. These photometric results demonstrate sustained light emission but should be distinguished from the controlled visibility and symbol-recognition assessment conducted using the PL paint. In that assessment, the formulated PL paint remained clearly visible for up to 90 min following a single 6 h sunlight charge. Overlapped tape regions also exhibited greater brightness than single-layer regions; however, because tape thickness and layer number were not systematically controlled, this observation represents preliminary evidence of a possible thickness-dependent effect rather than confirmation that layering extends functional visibility. Preliminary single-specimen environmental screening showed no visible coating failure following 24 h water immersion or the short temperature exposures used in this study. A dry-hard response was recorded at approximately 25 min and a later touch assessment at 12 h; these observations do not constitute a complete characterization of drying, curing or long-term serviceability. The present experiments do not demonstrate that double layering improves photoluminescent performance because the single- and double-layer datasets were obtained in separate campaigns without measured solar irradiance. Under real-world conditions, ambient stray light may offer occasional re-excitation, but it would also raise background luminance and reduce symbol contrast, so the visibility durations reported here, obtained in near-total darkness, should not be assumed to apply in service.

The potential practical applications identified from these findings should, however, be distinguished from effects that were directly demonstrated experimentally. The present study did not quantify reductions in electrically powered lighting demand, building energy consumption, or the environmental impacts associated with artificial light at night (ALAN), nor were the materials evaluated under full-scale operational conditions. Consequently, $SrAl_2O_4$:Eu^{2+},Dy^{3+} should at this stage be regarded as a potential zero-additional-operational-energy material for selected low-light, task-specific functions rather than as a demonstrated replacement for electrically powered lighting. Its ability to contribute to energy-demand reduction or reduced ALAN impacts will require validation through field-scale studies that compare PL systems with conventional lighting under representative operating conditions. Subject to such validation, the findings suggest two potential deployment routes. Adhesive-backed PL tape may be suitable for rapid demarcation and retrofit applications where installation simplicity is important. The greater brightness observed in overlapped regions also identifies material thickness and layering as variables for future controlled investigation rather than established design strategies. Acrylic-binder PL paint may offer a more geometrically flexible approach for surfaces such as steps, kerbs, handrail zones, columns, and signage backgrounds, where coating continuity and substrate conformance could be advantageous. These applications remain prospective and require further assessment under realistic charging, weathering, viewing, and operational conditions.

Author Contributions: Conceptualization, I.O., F.O.O. and D.-M.K.; data curation, I.O., C.L.O. and C.C.O.; formal analysis, F.O.O. and I.O.; funding acquisition, F.O.O., I.O., D.-M.K. and M.M.O.; investigation, C.C.O., and I.O.; methodology, I.O. and F.O.O.; project administration, F.O.O. and C.C.O.; supervision, I.O.; validation, F.O.O. and D.-M.K.; visualization, I.O. and F.O.O.; writing—original draft, I.O., C.L.O. and M.M.O.; writing—review and editing, F.O.O. and I.O. All authors have read and agreed to the published version of the manuscript.

Funding: This research received no specific grant from any funding agency in the public, commercial, or not-for-profit sectors.

Data Availability Statement: All data supporting the findings of this study are available within the article.

Conflicts of Interest: The authors declare no conflicts of interest.

References

1. Ogwu, I.; Long, Z.; Lee, D.; Zhang, X.; Zhang, W.; Okonkwo, M. Fundamental Issues in the Qualification of Smart and Intelligence in Building Materials Discourse: A Systematic Review. *Buildings* **2021**, *11*, 558. [CrossRef]
2. Okeke, F.O.; Ahmed, A.; Imam, A.; Hassanin, H. Harnessing the bio-structure of corncobs: Connecting morphology to mechanical attributes for sustainable building materials. *Clean Technol. Environ. Policy* **2026**, *28*, 70. [CrossRef]
3. Bibri, S.E.; Krogstie, J. Environmentally data-driven smart sustainable cities: Applied innovative solutions for energy efficiency, pollution reduction, and urban metabolism. *Energy Inform.* **2020**, *3*, 29. [CrossRef]
4. El-Khiary, A.M. Energy saving through smart buildings innovative technologies: Simulation analysis for evaluating smart material of energy performance in Egypt. *Int. J. Sustain. Build. Technol. Urban Dev.* **2021**, *12*, 232–250. [CrossRef]
5. Makakli, E.S. Potential of Smart Materials for Sustainable Architecture. *J. Acad. Soc. Sci. Stud.* **2024**, *2*, 267–275. [CrossRef]
6. Ogwu, I.; Okonkwo, M.; Agwu, K. Towards Zero Additional Energy Demand in Urban Built Environment Discourse. In *Proceedings of the 1st International Conference of the Faculty of Environmental Sciences*; Nnamdi Azikiwe University; Awka, Nigeria, 2024.
7. Rosso, F.; Fabiani, C.; Chiatti, C.; Pisello, A.L. Cool, photoluminescent paints towards energy consumption reductions in the built environment. *J. Phys. Conf. Ser.* **2019**, *1343*, 012198. [CrossRef]
8. Okeke, F.O.; Ahmed, A.; Imam, A.; Hassanin, H. A review of corncob-based building materials as a sustainable solution for the building and construction industry. *Hybrid. Adv.* **2024**, *6*, 100269. [CrossRef]
9. Kober, T.; Schiffer, H.-W.; Densing, M.; Panos, E. Global energy perspectives to 2060–WEC's World Energy Scenarios 2019. *Energy Strategy Rev.* **2020**, *31*, 100523. [CrossRef]
10. United Nations Climate Change. en.lighten Initiative|UNFCCC. Available online: https://unfccc.int/climate-action/momentum-for-change/activity-database/momentum-for-change-enlighten-initiative (accessed on 29 January 2026).
11. Climate Group. *Double Down on Energy Efficiency–Cut Costs, Build Jobs, Scale Innovation*; Climate Group: London, UK. Available online: https://www.theclimategroup.org/smart-energy (accessed on 29 January 2026).
12. Ibrahim, A.; Alsukkar, M.; Wang, L.; Hermaputi, R.L.; Dong, Y.; Yin, S.; Xiao, Y.; Hu, P. Targeting integrated daylighting comfort in deep office by multi-objective optimization using partial vertical deployment of adaptive corrugated shadings. *Energy Built Environ.* **2026**, *7*, 1556–1570. [CrossRef]
13. Mba, E.J.; Oforji, P.I.; Okeke, F.O.; Ozigbo, I.W.; Onyia, C.D.F.; Ozigbo, C.A.; Ezema, E.C.; Awe, F.C.; Nnaemeka-Okeke, R.C.; Onyia, S.C. Assessment of Floor-Level Impact on Natural Ventilation and Indoor Thermal Environment in Hot–Humid Climates: A Case Study of a Mid-Rise Educational Building. *Buildings* **2025**, *15*, 686. [CrossRef]
14. Lunn, R.M.; Blask, D.E.; Coogan, A.N.; Figueiro, M.G.; Gorman, M.R.; Hall, J.E.; Hansen, J.; Nelson, R.J.; Panda, S.; Smolensky, M.H.; et al. Health consequences of electric lighting practices in the modern world: A report on the National Toxicology Program's workshop on shift work at night, artificial light at night, and circadian disruption. *Sci. Total Environ.* **2017**, *607–608*, 1073–1084. [CrossRef] [PubMed]
15. Khan, Z.A.; Yumnamcha, T.; Mondal, G.; Devi, S.D.; Rajiv, C.; Labala, R.K.; Devi, H.S.; Chattoraj, A. Artificial Light at Night (ALAN): A Potential Anthropogenic Component for the COVID-19 and HCoVs Outbreak. *Front. Endocrinol.* **2020**, *11*, 622. [CrossRef] [PubMed]
16. Li, Z.; Jia, P.; Zhao, F.; Kang, Y. The Development Path of the Lighting Industry in Mainland China: Execution of Energy Conservation and Management on Mercury Emission. *Int. J. Environ. Res. Public Health* **2018**, *15*, 2883. [CrossRef] [PubMed]
17. Crnko, S.; Du Pré, B.C.; Sluijter, J.P.G.; Van Laake, L.W. Circadian rhythms and the molecular clock in cardiovascular biology and disease. *Nat. Rev. Cardiol.* **2019**, *16*, 437–447. [CrossRef] [PubMed]
18. Gaston, K.J.; Visser, M.E.; Hölker, F. The biological impacts of artificial light at night: The research challenge. *Philos. Trans. R. Soc. B Biol. Sci.* **2015**, *370*, 20140133. [CrossRef] [PubMed]
19. Wright, K.P.; McHill, A.W.; Birks, B.R.; Griffin, B.R.; Rusterholz, T.; Chinoy, E.D. Entrainment of the Human Circadian Clock to the Natural Light-Dark Cycle. *Curr. Biol.* **2013**, *23*, 1554–1558. [CrossRef] [PubMed]
20. Gradisar, M.; Wolfson, A.R.; Harvey, A.G.; Hale, L.; Rosenberg, R.; Czeisler, C.A. The Sleep and Technology Use of Americans: Findings from the National Sleep Foundation's 2011 Sleep in America Poll. *J. Clin. Sleep Med.* **2013**, *9*, 1291–1299. [CrossRef] [PubMed]
21. Paul, M. *Exposure to Artificial Light During Sleep May Increase Risk of Heart Disease and Diabetes*; News Center: Chicago, IL, USA, 2022. Available online: https://news.feinberg.northwestern.edu/2022/03/14/exposure-to-artificial-light-during-sleep-may-increase-risk-of-heart-disease-and-diabetes/ (accessed on 29 January 2026).
22. Kyba, C.C.M.; Kuester, T.; de Miguel, A.S.; Baugh, K.; Jechow, A.; Hölker, F.; Bennie, J.; Elvidge, C.D.; Gaston, K.J.; Guanter, L. Artificially lit surface of Earth at night increasing in radiance and extent. *Sci. Adv.* **2017**, *3*, e1701528. [CrossRef] [PubMed]
23. City of Toronto. *Best Practices for Effective Lighting*; City of Toronto: Toronto, ON, Canada, 2019. Available online: https://www.toronto.ca/city-government/planning-development/official-plan-guidelines/design-guidelines/best-practices-for-effective-lighting/ (accessed on 29 January 2026).

24. Hölker, F.; Moss, T.; Griefahn, B.; Kloas, W.; Voigt, C.C.; Henckel, D.; Hänel, A.; Kappeler, P.M.; Völker, S.; Schwope, A.; et al. The Dark Side of Light: A Transdisciplinary Research Agenda for Light Pollution Policy. *Ecol. Soc.* **2010**, *15*, 13. [CrossRef]
25. Falchi, F.; Cinzano, P.; Duriscoe, D.; Kyba, C.C.M.; Elvidge, C.D.; Baugh, K.; Portnov, B.A.; Rybnikova, N.A.; Furgoni, R. The new world atlas of artificial night sky brightness. *Sci. Adv.* **2016**, *2*, e1600377. [CrossRef] [PubMed]
26. Ferraro, V.; Settino, J. Evacuation and Smart Exit Sign System. In *The Internet of Things for Smart Urban Ecosystems*; Cicirelli, F., Guerrieri, A., Mastroianni, C., Spezzano, G., Vinci, A., Eds.; Springer International Publishing: Cham, Switzerland, 2019; pp. 363–383. [CrossRef]
27. Yen, H.-H.; Lin, C.-H. Intelligent Evacuation Sign Control Mechanism in IoT-Enabled Multi-Floor Multi-Exit Buildings. *Sensors* **2024**, *24*, 1115. [CrossRef] [PubMed]
28. 2012 International Building Code (IBC)-1024.2 Markings Within Exit Components. Available online: https://codes.iccsafe.org/s/IBC2012P13/chapter-10-means-of-egress/IBC2012P13-Ch10-Sec1024.2 (accessed on 29 January 2026).
29. NFPA 101 Code Development. Available online: https://www.nfpa.org/codes-and-standards/nfpa-101-standard-development/101 (accessed on 29 January 2026).
30. Kwong, Q.J. Light level, visual comfort and lighting energy savings potential in a green-certified high-rise building. *J. Build. Eng.* **2020**, *29*, 101198. [CrossRef]
31. Xiao, Y.; Pham, B.T.; Guo, M.-Z.; Ling, T.-C. Influence of luminescent powder type and characteristic on the glow light performance of architectural glass mortar. *J. Build. Eng.* **2022**, *58*, 105021. [CrossRef]
32. Al-Qahtani, S.D.; Al-Nami, S.Y.; Alkhamis, K.; Al-Ahmed, Z.A.; Binyaseen, A.M.; Khalifa, M.E.; El-Metwaly, N.M. Simple preparation of long-persistent luminescent paint with superhydrophobic anticorrosion efficiency from cellulose nanocrystals and an acrylic emulsion. *Ceram. Int.* **2022**, *48*, 6363–6371. [CrossRef]
33. *ASTM E2073-24*; Standard Test Method for Photopic Luminance of Photoluminescent (Phosphorescent) Markings. ASTM International: West Conshohocken, PA, USA, 2024. Available online: https://store.astm.org/e2073-24.html (accessed on 29 January 2026).
34. *DOT/FAA/AM-98/2*; Performance Demonstration of Zinc Sulfide and Strontium Aluminate Photoluminescent Floor Proximity Escape Path Marking Systems. Office of Aviation Medicine: Washington, DC, USA, 1998. Available online: https://libraryonline.erau.edu/online-full-text/faa-aviation-medicine-reports/AM98-02.pdf (accessed on 29 January 2026).
35. *DOT/FAA/AR-TN09/35*; Photoluminescent Material Evaluation. U.S. Department of Transportation: Washington, DC, USA, 2009. Available online: https://rosap.ntl.bts.gov/view/dot/90249 (accessed on 29 January 2026).
36. Floor Proximity Emergency Escape Path Marking Systems Incorporating Photoluminescent Elements. Available online: https://www.faa.gov/regulations_policies/advisory_circulars/index.cfm/go/document.information/documentid/22672 (accessed on 29 January 2026).
37. Grum, F.; Becherer, R.J. Optical Radiation Measurements. In *Radiometry*; Academic Press: San Diego, CA, USA, 1979; Volume 1.
38. Czyżewski, D. The Influence of a Photometric Distance on Luminance Measurements. *Energies* **2023**, *16*, 4166. [CrossRef]
39. *ASTM F963-16*; Standard Consumer Safety Specification for Toy Safety. ASTM International: West Conshohocken, PA, USA, 2016. [CrossRef]
40. Zhejiang Minhui Luminous Technology Co., Ltd. MHG—Yellow Green Strontium Aluminate Photoluminescent Pigment. Available online: https://www.mphotoluminescent.com/mh-g-series-aluminate-based.html (accessed on 29 January 2026).
41. Standard Test Methods for Evaluating Drying or Curing During Film Formation of Organic Coatings Using Mechanical Recorders. Available online: https://store.astm.org/d5895-20.html (accessed on 29 January 2026).
42. *GB/T 1728-1979*; Methods of Test for Drying Time of Coatings of Paints and Putties. National Technical Committee for Standardization of Coatings and Pigments: Beijing, China, 1979.
43. Standard Practice for Testing Water Resistance of Coatings Using Water Immersion. Available online: https://store.astm.org/d0870-15r20.html (accessed on 29 January 2026).
44. *GB/T 1733-1993*; Determination of Resistance to Water of Films. National Standard of the People's Republic of China: Beijing, China, 1993. Available online: https://www.chinesestandard.net/PDF.aspx/GBT1733-1993 (accessed on 29 January 2026).
45. Bi, Y.; Pei, J.; Chen, Z.; Zhang, L.; Li, R.; Hu, D. Preparation and characterization of luminescent road-marking paint. *Int. J. Pavement Res. Technol.* **2021**, *14*, 252–258. [CrossRef]
46. *CIE S 025/E:2015*; Test Method for LED Lamps, LED Luminaires and LED Modules. CIE: Vienna, Austria, 2015.
47. Zeng, P.; Wei, X.; Yin, M.; Chen, Y. Investigation of the long afterglow mechanism in SrAl2O4:Eu2+/Dy3+ by optically stimulated luminescence and thermoluminescence. *J. Lumin.* **2018**, *199*, 400–406. [CrossRef]
48. Kalkal, K.; Dwivedi, Y. Engineering Persistent Luminescence in SrAl2O4:Eu2+, Dy3+ for Signage Application. *J. Electron. Mater.* **2025**, *54*, 8372–8384. [CrossRef]
49. Koizumi, R.; Takahashi, R.; Yamada, S.; Hattori, S.; Shinozaki, K. Visualization of trap distribution in SrAl2O4:Eu2+,Dy3+ revealed by simulations of luminescence changes in charging and emission of persistent luminescence and thermoluminescence based on a random walk model. *Phys. Chem. Chem. Phys.* **2025**, *27*, 15850–15857. [CrossRef] [PubMed]

50. Botterman, J.; Smet, P.F. Persistent phosphor $SrAl_2O_4$:Eu,Dy in outdoor conditions: Saved by the trap distribution. *Opt. Express* **2015**, *23*, A868–A881. [CrossRef] [PubMed]
51. Osmi, S.K.C.; Munikanan, V.; Husen, H.; Suif, Z.; Othman, M.; Ahmad, N.; Rizal, N.A.S. Characteristics of Photo-Luminescent (pl) Powder Applied with Polyester Resin as Glow-in-the-Dark Emergency Signage. *Zulfaqar J. Def. Sci. Eng. Technol.* **2020**, *3*, 32–38. [CrossRef]

Disclaimer/Publisher's Note: The statements, opinions and data contained in all publications are solely those of the individual author(s) and contributor(s) and not of MDPI and/or the editor(s). MDPI and/or the editor(s) disclaim responsibility for any injury to people or property resulting from any ideas, methods, instructions or products referred to in the content.